AGU PUBLICATIONS

JGR

Journal of Geophysical Research: Atmospheres

RESEARCH ARTICLE
10.1002/2016JD025002

**Key Points:**
- Irrigation vigor negatively impacts precipitation
- Irrigation vigor negatively impacts temperature
- Irrigation negatively impacts fronts and heat wave threshold

**Supporting Information:**
- Supporting Information S1
- Figure S1
- Figure S2
- Figure S3
- Figure S4

**Correspondence to:**
C. Selman,
cms05j@my.fsu.edu

**Citation:**
Selman, C., and V. Misra (2016), The sensitivity of southeastern United States climate to varying irrigation vigor, *J. Geophys. Res. Atmos.*, *121*, doi:10.1002/2016JD025002.

Received 26 FEB 2016
Accepted 16 JUN 2016
Accepted article online 19 JUN 2016



# The sensitivity of southeastern United States climate to varying irrigation vigor

**Christopher Selman[1,2] and Vasubandhu Misra[1,2,3]**

[1]Department of Earth, Ocean and Atmospheric Science, Florida State University, Tallahassee, Florida, USA, [2]Center for Ocean-Atmospheric Prediction Studies, Florida State University, Tallahassee, Florida, USA, [3]Florida Climate Institute, Florida State University, Tallahassee, Florida, USA

**Abstract** Four regional climate model runs centered on the Southeast United States (SEUS) assuming a crop growing season of May through October are irrigated at 25% (IRR25), 50% (IRR50), 75% (IRR75), and 100% (IRR100) of the root zone porosity to assess the sensitivity of the SEUS climate to irrigation. A fifth run, assuming no irrigation (CTL), is used as the basis for comparison. Across all IRR runs, it is found that there is a general reduction in seasonal mean precipitation over the irrigated cells relative to CTL. This manifests as an increase in dry (0–1 mm/d) days and reduction in $>1$ mm/d rainfall events. A comparative moisture budget reveals that area-averaged precipitation over the irrigated cells displays a reduction in precipitation and runoff in IRR100 with a weaker reduction in IRR25. This is despite an increase in vertically integrated moisture convergence and local evaporation. We find that irrigation increases the lower atmospheric stability, which in turn reduces the convective rainfall over the irrigated areas. Seasonally averaged temperatures reduce over irrigated areas, with the intensity of the reduction increasing with irrigation vigor. This is largely attributed to a repartitioning of sensible heat flux into latent heat flux. There is also, however, a small increase of heat flow to deeper soil layers. Precipitation ahead of transient cold fronts is also reduced by irrigation as they pass over irrigated cells, owing to the increased stability in the lower troposphere. The intensity of this precipitation reduction becomes more intense as irrigation vigor increases. Lastly, heat waves in the SEUS are reduced in intensity over irrigated cells.

## 1. Introduction

Irrigation plays a role in modulating regional and global climate [*Puma and Cook,* 2012; *Sacks et al*., 2009]. As such, it becomes crucial that atmospheric global climate models (AGCMs) incorporate land use features into their simulations [*Marcella and Eltahir,* 2014]. However, AGCMs presently offer too coarse a resolution to capture the region-specific impacts of irrigation, necessitating the use of higher-resolution, regional models. These models, owing to their higher grid size resolution, are able to better capture small, mesoscale phenomena and fine scale land-atmosphere interactions by better resolution of surface inhomogeneities and convective characteristics [*Jacob et al*., 2014]. One such consideration that must be made in simulations is the application of irrigation, which has notable potential impacts on local land-surface processes [*Selman*, 2015].

Irrigation's impacts are broad and region specific. Using the Massachusetts Institute of Technology Regional Climate Model modified to irrigate with a water mass conservation scheme, *Im and Eltahir* [2014] noted that irrigation responses further exhibit a strong latitudinal dependence. Temperature changes were seen to be as large as 10°C in some areas, while other areas exhibited little change [*Lobell et al*., 2009]. It was shown that the magnitudes of these changes were primarily determined by fractional area equipped for irrigation, model cloud considerations and biases in soil moisture [*Cook et al*., 2015]. Irrigation further impacts the thermal budget of a region, particularly adjusting the Bowen ratio to favor latent heating over sensible heating [*Cook et al*., 2015]. Irrigation has also been implicated in fundamentally altering the South Asian summer monsoon [*Saeed et al*., 2009; *Shukla et al*., 2014] by reducing land/sea temperature contrasts. Further, as agriculture in the Indian subcontinent continues to grow, stronger irrigation and greenhouse gas contributions can result in a 40% reduction in the interannual variability of the South Asian summer monsoon [*Shukla et al*., 2014]. In the California Central Valley, irrigation strengthens the water cycle [*Lo and Famiglietti*, 2013], cools daytime maximum temperatures and warms nighttime minimum temperatures [*Kanamaru and Kanamitsu*, 2008]. The Southeast United States (SEUS), unlike the semiarid regions of the Southwest U.S., has been identified as a region with strong soil moisture memory, persisting up to 10 months in a flood irrigation setup [*Hagemann and Stacke*, 2015]. Soil moisture-precipitation coupling can also be affected in irrigated regimes [*Misra and Dirmeyer*, 2009; *Wei and Dirmeyer*, 2012]. Irrigation can also manifest in lowering planetary boundary layer

(PBL) heights in dry areas [*Kueppers and Snyder*, 2012] by as much as 500 m, causing a significant reduction in precipitation [*Marcella and Eltahir*, 2014]. PBL height reductions are attributed to reductions in average daily temperatures on the order of 0.5°C to 1.0°C in both West Africa [*Marcella and Eltahir*, 2014] and the SEUS [*Selman*, 2015]. Further, this reduction in precipitation can serve to enhance local subsidence and foster low-level anticyclonic circulation in a region [*Im et al*., 2014]. These impacts have been noted to be primarily local to the irrigated areas [*Sorooshian et al*., 2011].

Irrigation influences precipitation in many ways, which again exhibit a regional dependence. In the Texas Panhandle, in the presence of synoptic conditions, which favor precipitation development, irrigation was found to increase overall rainfall in an area [*Barnston and Schickedanz*, 1984]. Such synoptic conditions included stationary and cold fronts, with a strong preference toward the month of June for most pronounced impacts and produced slightly lower lifted indices in the region. In the American Midwest, *Alter et al.* [2015] found an observational relationship between summer precipitation intensity and frequency, and enhanced irrigation. This is attributed largely to irrigation increasing the frequency and intensity of precipitation downwind of irrigated areas. They speculate that features such as precipitation recycling and sea breeze-like circulations induced by differed surface characteristics may be at play in altering precipitation. This corroborates a similar study by *DeAngelis et al.* [2010], which noted an irrigation-induced increase in precipitation over the Great Plains.

Modeling studies have also indicated that irrigation impacts precipitation. Using the Weather Research and Forecasting (WRF) model that used the NOAH land surface model (LSM) [*Ek et al*., 2003] and observed fractional irrigation data, *Harding and Snyder* [2012] simulated an increase in precipitation over the Great Plains both above and downwind of irrigated areas. *Qian et al.* [2013] implemented a more operational-like irrigation scheme in WRF, which uses observed fractional irrigation data disaggregated to the model domain. A greenness fraction threshold is specified, and should the model meet this threshold, irrigation is triggered when root-zone soil moisture falls below 50%. Changes in precipitation are found to be inhomogeneous over the Southern Great Plains, with only a slight increase found in the areal average. Recalling that irrigation has subregion dependent results, we must note here that drivers of convective activity in the SEUS are quite different from other regions. In the SEUS, convection is primarily driven by either a diurnally oscillating sea breeze [*Schwartz and Bosart*, 1979] in coastal areas or mountain-crossing mesoscale complex systems from the central United States [*Parker and Ahijevych*, 2007]. Because of those features, and the overall moist climate of the area, there is a strong possibility that irrigation impacts in the SEUS will be different from those in the Great Plains.

In the SEUS, irrigation is not common. Florida, on average, withdraws about one to five billion gallons of water per day in 2005 [*Hutson et al*., 2000]. Other areas, for instance, the California Central Valley, withdraw 10 times as much. The primary reason for this difference is in the local climatology; the Central Valley of California is functionally an arid climate (yet remains an agricultural hotbed) [*McNally et al*., 2004]. The SEUS, however, is humid and subtropical, ensuring constant delivery of summer rainfall for crop-growing purposes. Despite this advantage over California, agriculture remains a modest industry valued at $11 billion in the SEUS (Data taken from the United States Department of Agriculture's Environmental Research Survey). If present trends in California drought continue, there may be added pressure on the SEUS agriculture industry to produce more vigorously to compensate for the shortfall in the agricultural productivity [*Alston et al*., 2010; *McNider et al*., 2005; *McNider and Christy,* 2007]. As demand for water increases, so too will the need for intelligent water management policies, irrigation included. In fact, this sort of increase in irrigation has been observed, with Georgia, Alabama, and Mississippi having the largest increases in irrigated water usage and acreage since 1998 in the eastern United States [*Schaible and Aillery*, 2012]. This increase in irrigation is owed primarily to both a growth in agricultural industries and risk avoidance due to reoccurring drought conditions [*Evett et al*., 2003; *Vories and Evett,* 2010],

Should these trends continue, adoption of irrigation may have an impact on SEUS climate. For example, *Misra et al.* [2012] found that long-term temperature trends are affected by irrigation in the SEUS. However, when different crops are grown, then they are irrigated with varying vigor, requiring investigation into how sensitive the climate of the SEUS is to such variations in irrigation. In this study, we propose an analysis that assumes four unique 10 year integrations with irrigation set at different root-zone soil moisture contents. This analysis comprises mainly of a comparative analysis of the sensitivity of the regional climate of SEUS to irrigation vigor with respect to a control integration from the same model but without any implementation of irrigation. This control integration has been extensively discussed and validated in *Selman and Misra* [2015].

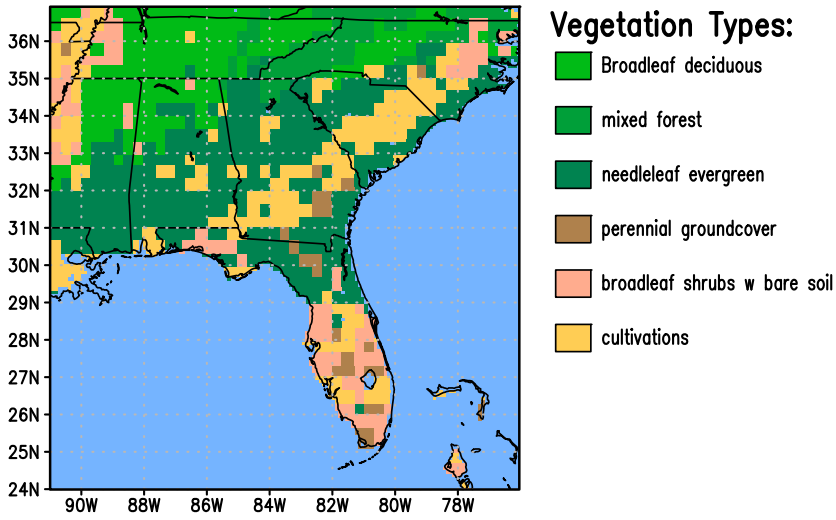


**Figure 1.** Region used in this study, broken down by vegetation type. Irrigation is applied to cells denoted as cultivations.

## 2. Data and Methods

For the purposes of this study, we used the Regional Spectral Model (RSM) [*Kanamitsu et al*., 2010], at a horizontal resolution of 10 km. The regional domain is depicted in Figure 1. The RSM has been demonstrated to reasonably simulate the dominant mechanisms of precipitation in the SEUS [*Selman and Misra*, 2015] when using the Kain-Fritsch cumulus parameterization scheme [*Kain and Fritsch*, 1993]. Further, the RSM is not sensitive to choice of domain owing to its use of scale selective bias correction [*Kanamaru and Kanamitsu*, 2007]. Because of this feature we are able to downscale directly from the ~250 km resolution of the National Centers for Environmental Prediction Reanalysis 2 (NCEP-R2) [*Kanamitsu et al*., 2002] to the model's 10 km horizontal resolution. The NCEP-R2 data set was chosen for boundary conditions over the integration period 1989–1999. For purposes of our analyses, the first year is discarded as model spin up.

Critical to our analyses was the choice of the LSM. We chose to use the NOAH LSM [*Ek et al*., 2003], modified for irrigation specification. It parameterizes land surface use by classifying surface types into the 12 vegetation types of the simplified biosphere model [*Loveland et al*., 1995] and the 8 soil types of *Zobler* [1986]. The NOAH LSM was modified to allow user specification of growing season (in months) and irrigation vigor (in fraction of field capacity of the root zone). Irrigation is applied to two subsurface layers over the cultivated cells (Figure 1), spanning 10–100 cm depth, mimicking a subirrigation process that allows for both addition and drainage of soil moisture. Added (removed) irrigation moisture is constrained to never exceed (fall below) porosity (wilting point). The irrigation process is summarized in Figure 2. The simplicity of this method is a consequence of the static vegetation characteristics of the model; crucial variables such as leaf area index, greenness fraction, and soil heat capacity are not dynamic within the RSM, limiting our potential choices for irrigation schema. That said, this method is on par with other irrigation studies using the RSM [e.g., *Kanamaru and Kanamitsu*, 2008] and is enhanced by our implementation of irrigation, which also tracks the amount of water being employed for irrigation.

To assess the sensitivity of SEUS climate to irrigation, we perform four independent model runs, fixing the 10–100 cm soil layer to 25%, 50%, 75%, and 100% of saturation (or porosity) in IRR25, IRR50, IRR75, and IRR100, respectively. A fifth model run, with no irrigation modification, is also produced (CTL) which follows from *Selman and Misra* [2015]. We then analyze each model's simulated output against CTL in order to determine the changes relative to each integration. Our CTL run has been extensively validated against both NCEP Stage IV radar observations [*Lin and Mitchell,* 2005] and North American Land Data Assimilation System (NLDAS) temperature forcing data [*Selman and Misra,* 2015]. It was found that by using any combination of either NCEP-R2, European Center ERA-40 [*Uppala et al*., 2005] as lateral boundary conditions and Kain-Fritsch or Relaxed Arakawa Schubert convection scheme, the model verifies quite well against observation. In particular, it does a reasonable job in simulating magnitude and phase of the diurnal amplitude of both precipitation and temperature (both are significant contributors to the overall climatology of the SEUS [*Bastola and Misra,* 2013; *Selman et al*., 2013; *Selman and Misra,* 2015]) and keeps the root-mean-square error (RMSE) reasonably

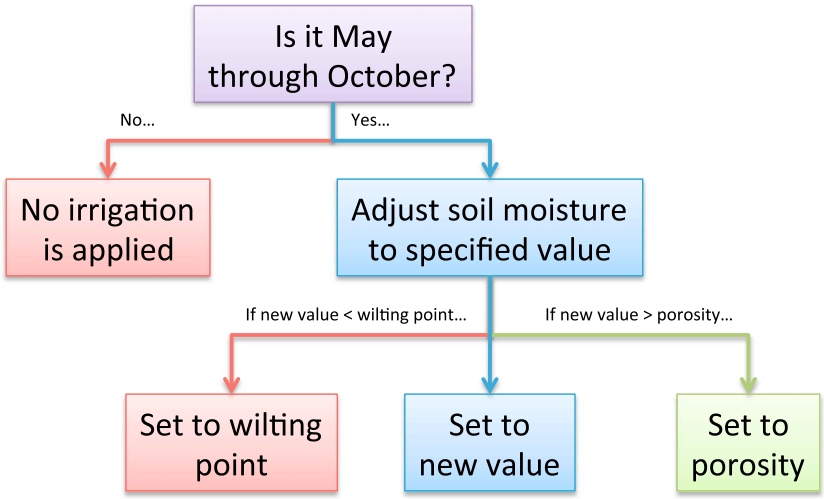


**Figure 2.** Flowchart outlining the irrigation process used in this study.

small relative to the observations. Additional details of these results, the fidelity of the CTL integration, as well as a sensitivity analysis of parameterization choices can be found in *Selman and Misra* [2015]. We depict from this analysis the fidelity of our CTL run's depiction of diurnal precipitation and temperature (Figures S1 and S2 in the supporting information) relative to Stage IV rainfall observations [*Lin and Mitchell*, 2005] and NLDAS-1

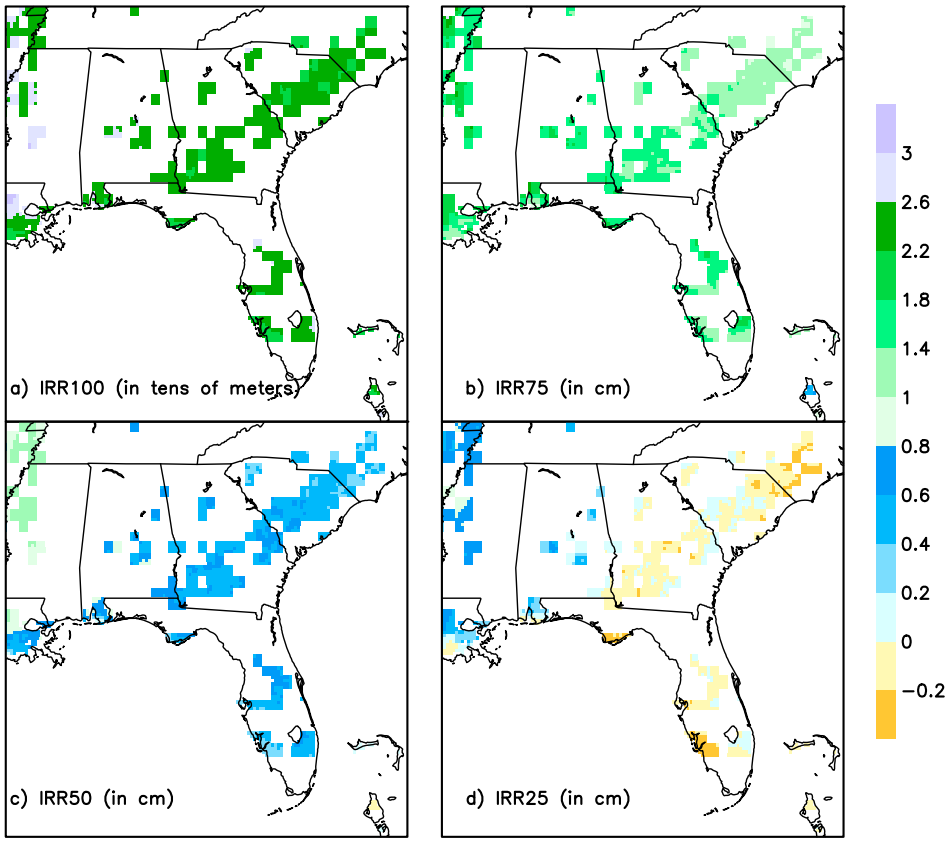


**Figure 3.** Depth of water added to each cell in order to reach (a) 100%, (b) 75%, (c) 50%, and (d) 25% of porosity. Units are expressed in centimeters in all panels except in Figure 3a which is in tens of meters. All panels use the same color scale as indicated.

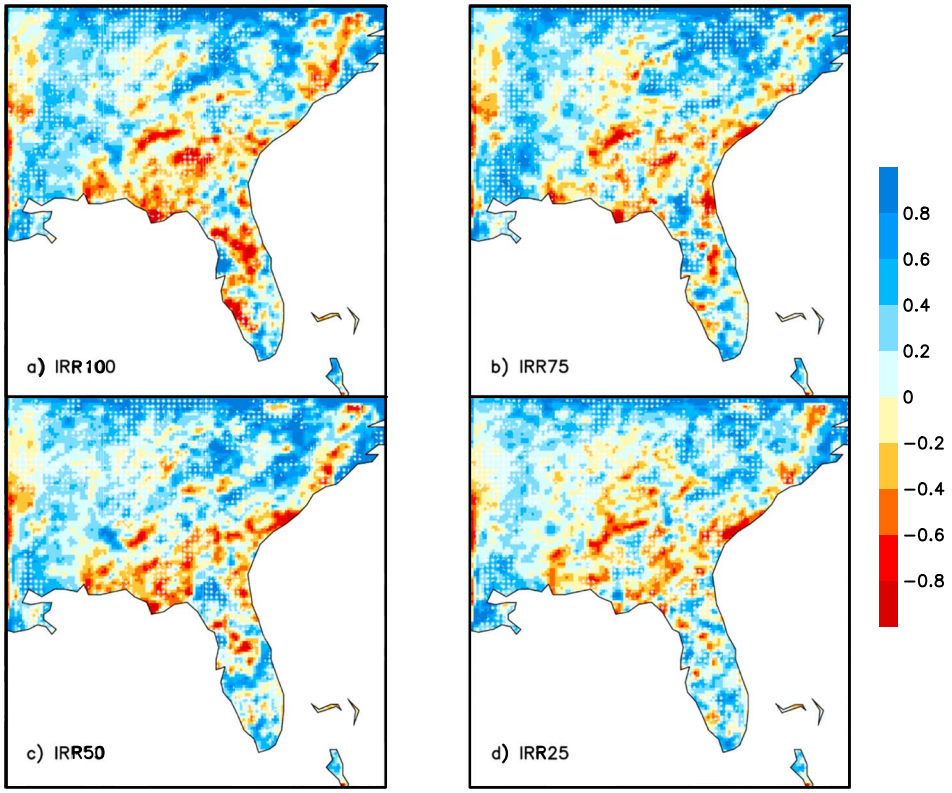


**Figure 4.** Change in seasonal average precipitation (IRR-CTL; mm $d^{-1}$), maintaining field root-zone soil moisture at (a) 100%, (b) 75%, (c) 50%, and (d) 25% of porosity. Stippling indicates changes significant at the 10% confidence interval.

[*Cosgrove et al.*, 2003] temperature forcing. In general, over the growing season, depiction of the relative error of temperature and precipitation is not within 1 standard error of observation. However, simulation of the phase of the diurnal maximum precipitation and temperature are quite good, especially in summer months, indicating that the timings of dominant drivers are well-represented within the model.

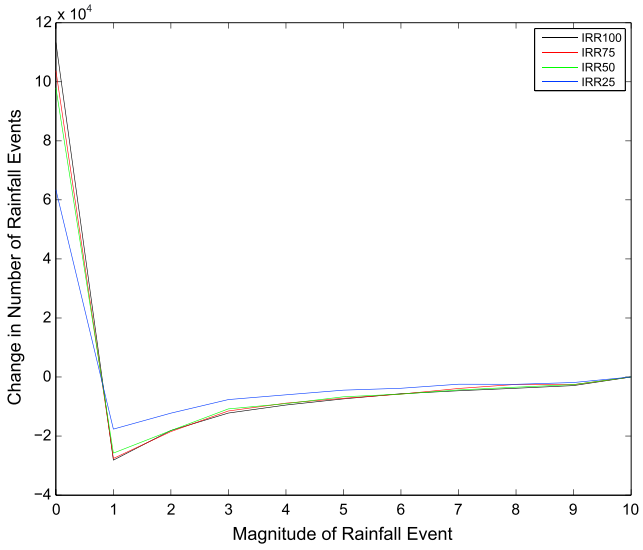


**Figure 5.** Climatological difference (IRR-CTL) in total number of rainfall events binned in 1 mm/d intervals, aggregated over irrigated cells. Units of the ordinate axis are in days.

## 3. Results

In keeping the soil moisture fixed to 100%, an unrealistic depth of water was used (Figure 3a). This is in stark contrast to the lower percentages (IRR25, IRR50, and IRR75), which use a depth measured in the tens of millimeters. The high withdrawal values are primarily a result of irrigation being applied at all hours throughout the season (May–October) rather than short concentrated bursts during the day. In the intermediate levels of irrigation of IRR75 (Figure 3b) and IRR50 (Figure 3c) far less water is withdrawn to irrigate compared to IRR100. It may

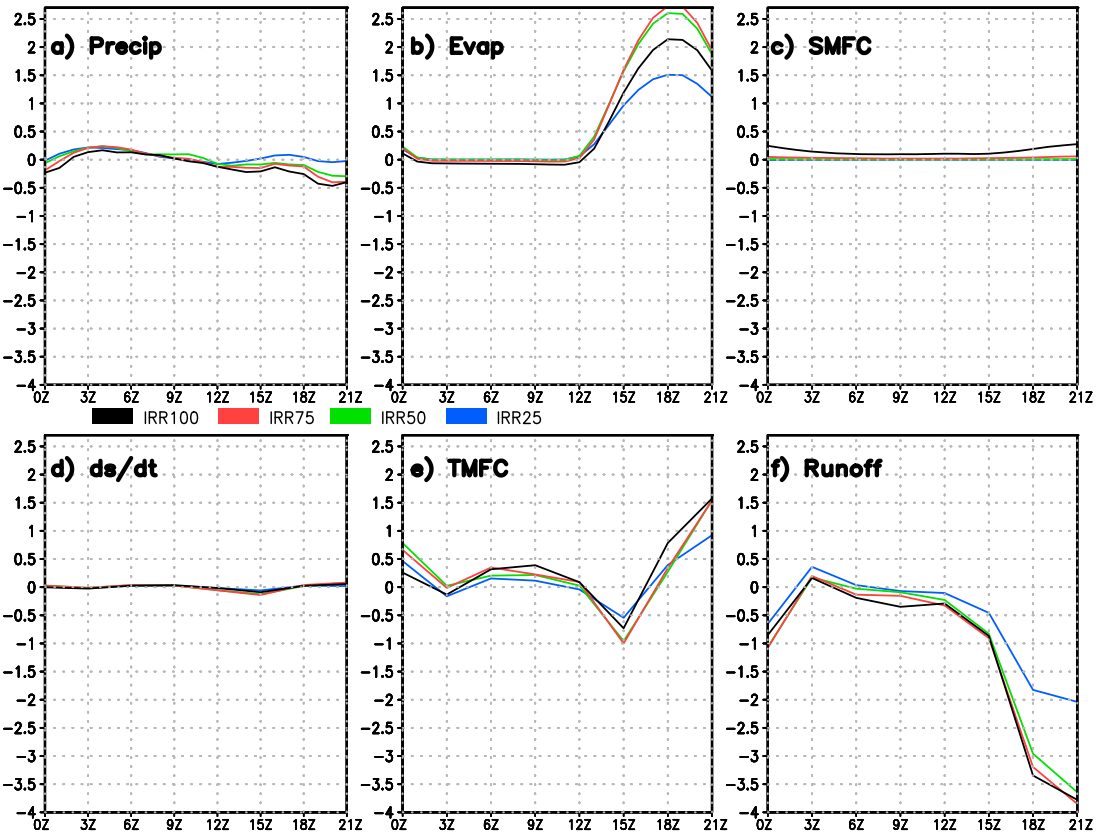


**Figure 6.** Climatological difference of irrigation runs from CTL of the area-averaged terms of the moisture budget. Units are in mm/d. The blue line is IRR25, the green line is IRR50, red is IRR75, and black is IRR100. Panels represent (a) precipitation (PCP), (b) evaporation (EVAP), (c) vertically integrated stationary moisture flux convergence (SMFC), (d) change in column precipitable water (d*s*/d*t*), (e) transient moisture flux convergence (TMFC), and (f) runoff (Runoff). Transient moisture flux convergence is computed as a residual. Units are in mm/h.

be noted that in IRR25 (Figure 3d), soil moisture is being drained out of the irrigated cells in the mean, unlike the other irrigation experiments. However, the values in Figure 3 still highlight an important aspect of irrigation being applied to the SEUS: despite a primarily rain-fed agricultural system, considerable amounts of water must be applied to maintain soil moisture at porosity.

### 3.1. Impact on Seasonal Rainfall

Qualitatively, in an overall sense, irrigation seems to negatively impact rainfall over irrigated cells during the irrigated season (Figure 4). We performed a Monte Carlo statistical significance test [*Wilkes*, 2011] to determine which regions were experiencing a statistically significant change. Over the irrigated cells, the reduction in precipitation is found to be statistically significant. However, the pattern of decrease in precipitation over the irrigated cells in Figure 4 is seen to be quite heterogeneous and noisy, so a more quantitative approach is required to fully assess the change. We compute the areal average over irrigated cells and find that precipitation decreases by 0.11 mm/d in IRR100 and 0.06 mm/d in IRR75, has a negligible decrease in IRR50, and has a negligible increase in IRR25. This implies an inverse sensitivity to irrigation vigor; the strongest irrigation serves to reduce precipitation over the irrigated cells while slightly enhancing precipitation in the weakest incidences of irrigation vigor. This diversity of results from variation of irrigation vigor will be further expanded upon in the subsequent subsections.

Irrigation reduces precipitation in two primary ways: by increasing the number of dry days and reducing the number of $>1$ mm/d events (Figure 5). The decrease in magnitude of the change in number of dry days follows irrigation vigor quite nicely, with IRR100 seeing the largest increase in 0–1 mm/d rainfall events (or dry days) and the change steadily decreasing until IRR50. In IRR25 there is an increase in dry days, which is

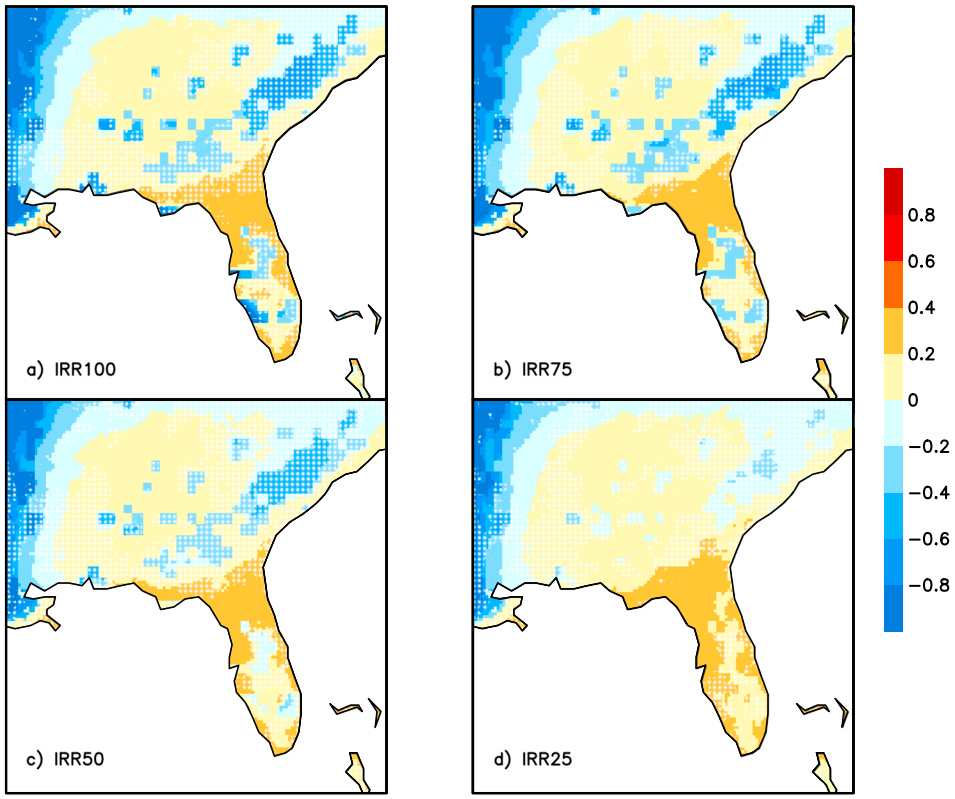


**Figure 7.** Change in seasonal average temperature (IRR-CTL), maintaining field root zone soil moisture at (a) 100%, (b) 75%, (c) 50%, and (d) 25% of porosity. Stippling indicates changes significant at the 10% confidence interval.

roughly 50% that of IRR100. This pattern persists into the 1–4 mm/d range, with IRR100 seeing the largest reduction, and a substantial separation between IRR50 and IRR25. This noticeable jump could likely be related to the drainage of soil moisture in the IRR25 run (Figure 3d), a feature not seen in any of the other three simulations. We note here that the results of IRR25 are somewhat counterintuitive; in Figure 3 above, we noted that IRR25 produces an average drainage of water. As such we would expect the results of IRR25 to be opposite that of the other model runs. This is an example of a situation were a seasonal average is somewhat misleading. Irrigation water is primarily drained in the off-diurnal peak hours and added during the afternoon hours (not shown). Because this water is added at the diurnal peak, the concomitant changes in precipitation and other fields (shown later) are in line with the other experiments.

We have also analyzed the differences in the moisture budget (Figure 6) (averaged over all irrigated cells) to determine if any particular term exhibits sensitivity to varied irrigation vigor. The moisture budget is computed as

$$\frac{\partial Q}{\partial T} = -\nabla \cdot M + E - P - R \tag{1}$$

The moisture flux convergence term ($-\nabla \cdot M$) is broken down into two components: stationary moisture flux convergence and transient moisture flux convergence terms. The transient moisture flux convergence term is computed as a residual of the moisture budget in equation (1). Throughout the day, precipitation is again seen to reduce relative to CTL (Figure 6a) with a very slight increase in precipitation in the late afternoon and during the evening hours of IRR25. However, as irrigation vigor increases, precipitation magnitude further decreases, with a considerable decrease between 18 and 21 UTC. Changes in evaporation (Evap; Figure 6b) are less obvious; though there appears to be a general increase as irrigation vigor increases. However, at diurnal peak, IRR100 drops below IRR75 and IRR50. This is related to a reduction in the humidity gradient between the surface and lowest model level over the irrigated cells (not shown) and precipitation (Figure 6a), which reduces precipitation recycling at diurnal peak. Vertically integrated stationary moisture

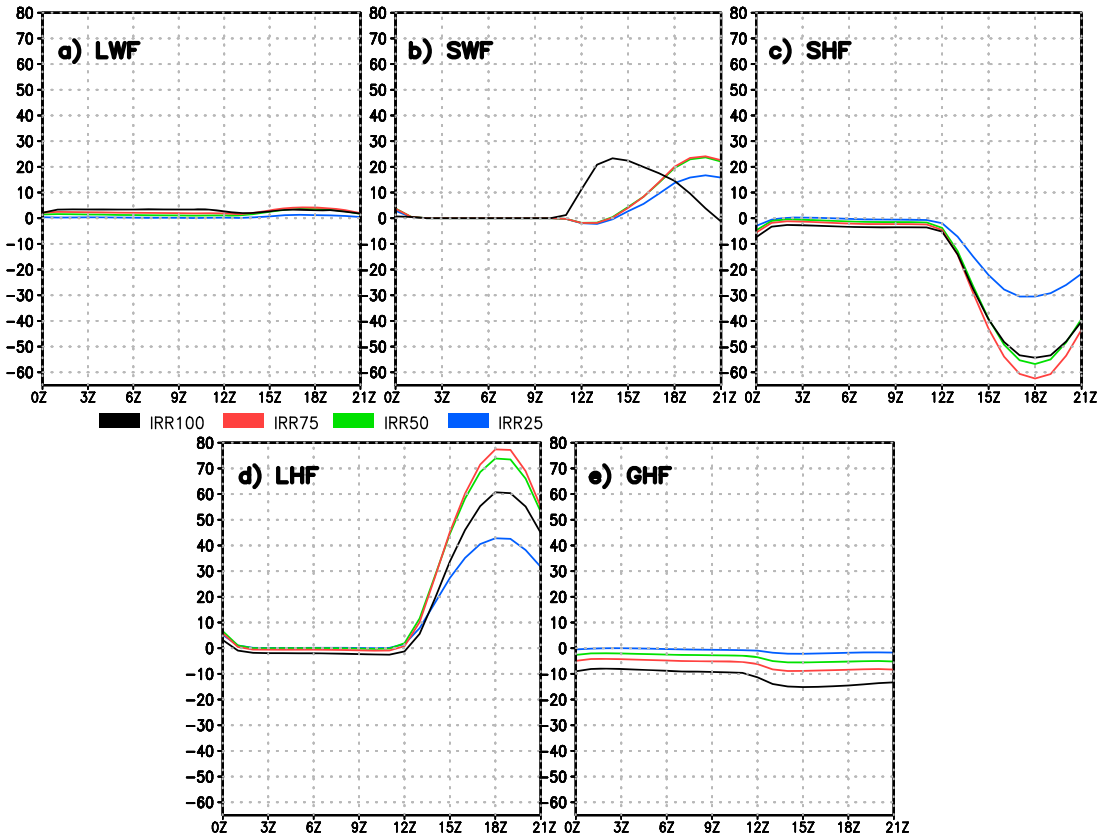


**Figure 8.** Difference of irrigation area-averaged terms of the heat budget from CTL. Terms are represented as (a) net longwave flux (LWF), (b) net shortwave flux (SWF), (c) sensible heat flux (SHF), (d) latent heat flux (LHF), and (e) ground heat flux (GHF). The sign of each flux follows meteorological conventions. Units are in $W/m^2$. The blue line is IRR25, the green line is IRR50, the red line is IRR75, and the black line is IRR100.

flux convergence (SMFC; Figure 6c) represents a small portion of the moisture budget's difference between the IRR and CTL experiments but nonetheless exhibits sensitivity to irrigation vigor. The afternoon and evening peaks in stationary moisture flux convergence (SMFC) increase in magnitude as irrigation vigor is increased (Figure 6c). The transient moisture flux term (TMFC) also exhibits an overall increase over irrigated areas but has no clear sensitivity associated with irrigation vigor. In the case of runoff (Figure 6f) there is a proportionate decrease relative to CTL around the diurnal peak (18–21 UTC) values. This reduction in the runoff is consistent with the corresponding decrease in rainfall with irrigation.

We note here that a reduction in precipitation would be quite paradoxical with coincident rise in diurnal peak of stationary and transient moisture flux convergence and local evaporation. This paradox is explained by an overall stabilization of the atmosphere over irrigated cells. *Selman* [2015] find that in IRR100 the excessive irrigation causes, through local cloud radiation feedback, stabilization of the lower atmospheric column that results in the reduction of the precipitation over the irrigated cells. In Figure 5 we clearly observed that the irrigation has a greater impact on the weak rain events compared to the moderate to strong events. This is because of the stabilization of the lower atmosphere during the evening and morning hours (Figures S3 and S4) caused by the cooling of the surface, which results in a higher barrier for convection to initiate during the diurnal peak of precipitation. On the other hand, stronger rain events can overcome the increased stability offered by irrigation in the presence of strong convective forcing.

### 3.2. Impact on Seasonal Temperatures

Irrigation is also seen to have an impact on seasonally averaged surface temperatures (Figure 7). There is a pronounced reduction in seasonally averaged surface temperature across all months in all IRR simulations, especially those over 25% of porosity. As with precipitation, we perform a Monte Carlo statistical significance

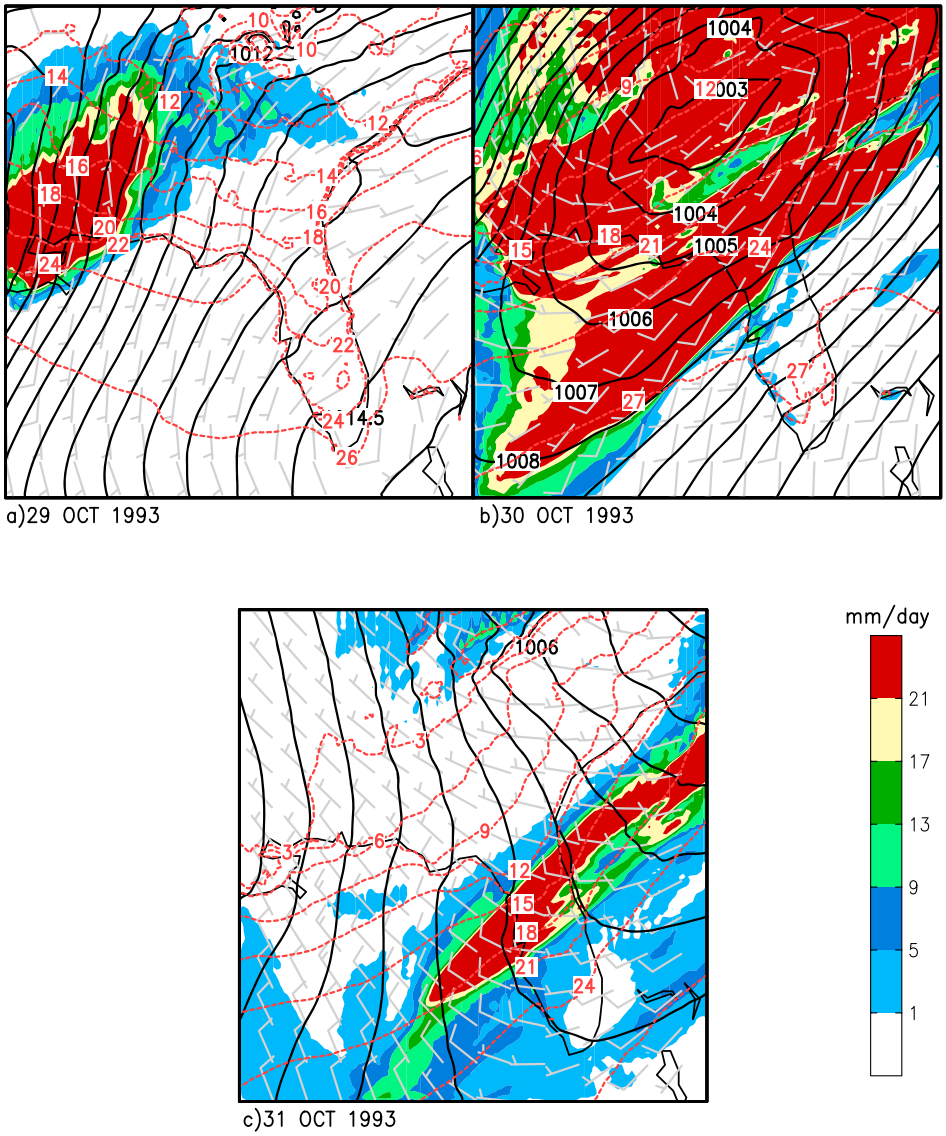


**Figure 9.** Conditions (a) 1 day before, (b) during, and (c) 1 day after a typical late October frontal passage over the SEUS from CTL. Underlaid wind barbs are in knots, dashed and red contours indicate isotherms, solid lines indicate mean sea level pressure, and shading indicates precipitation intensity.

test [*Wilkes*, 2011] to confirm that these reductions are significant. Surface temperature reductions are seen to be primarily local to the irrigated areas. The intensity of the reduction follows irrigation vigor; for instance, in IRR25 (Figure 7d) there is no significant decrease in surface temperature stemming from irrigation. But as irrigation vigor increases so too does the magnitude of the surface temperature reduction (Figures 7a, 7b, and 7c). The large areas of statistically insignificant cooling present on the western boundary are an artifact of the lateral boundary conditions being shocked to 25–100% capacity from a lower soil moisture value and do not reflect the processes occurring in the interior of the domain.

We can break down the surface heat budget to determine where excess energy is being transferred (Figure 8). In contrast to the moisture budget, all terms of the heat budget seem to exhibit consistent sensitivity to irrigation vigor. For instance, net longwave radiative flux (LWF; Figure 8a) appears to change by about 1 W/m$^2$ with respect to CTL between each of IRR25 through IRR100 experiments. The net positive adjustment to longwave flux indicates that more energy escapes from the surface as irrigation vigor increases. Similarly shortwave flux (SWF; Figure 8b) increases across all irrigated runs, though the differences between runs seem to be less

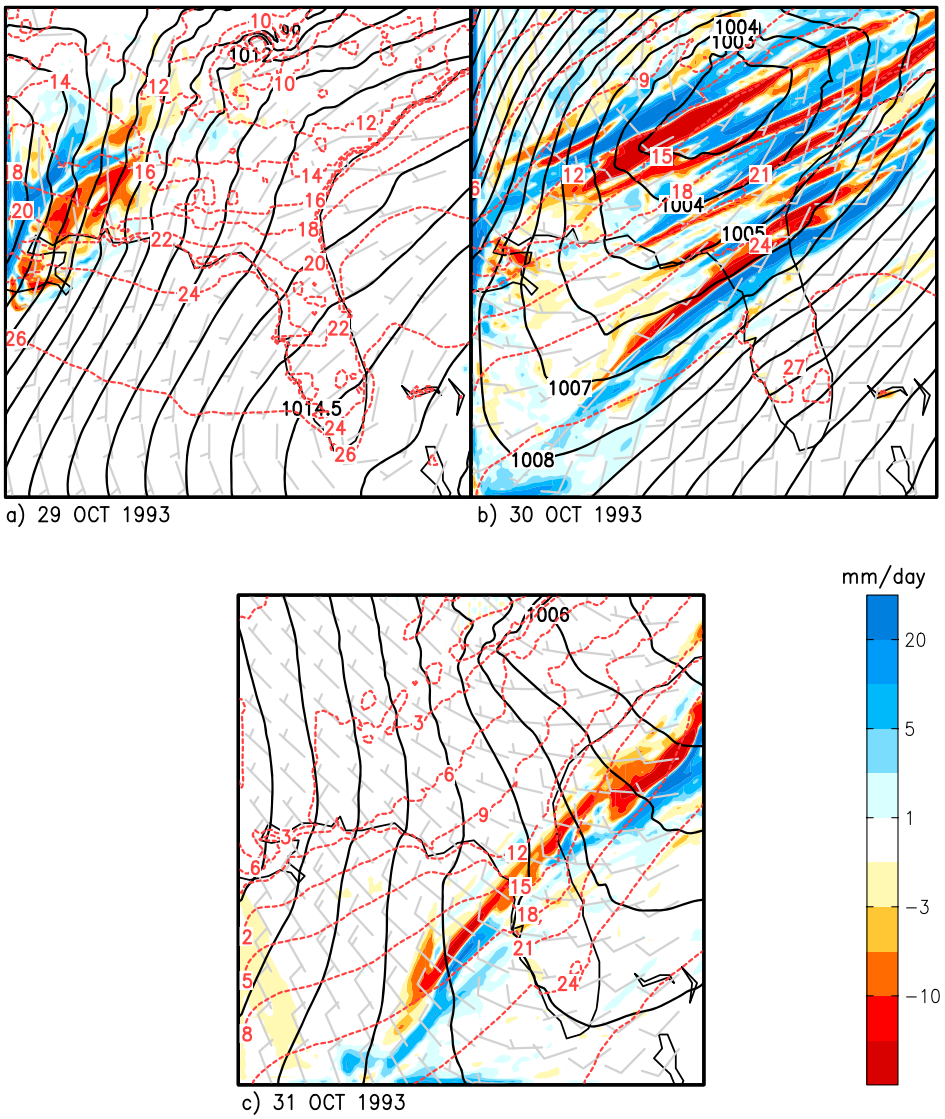


**Figure 10.** As in Figure 9 but precipitation is plotted as a difference in IRR100 rainfall relative to CTL.

apparent than for LWF. Sensible heat flux (SHF; Figure 8c) decreases as irrigation vigor increases, but this relationship is nonlinear. That is, the reduction in SHF is disproportionate to the increase in irrigation vigor. Furthermore, there is a nonlinear increase in latent heat flux with irrigation vigor (LHF; Figure 8d). This is to be expected from our analysis of the moisture budget, in which evaporation was seen to increase in the irrigated runs (Figure 6b). There is a strong diurnal cycle in the changes in LHF/SHF that merits discussion. Daytime changes near the diurnal peak are quite large, owing to the excess availability of moisture supplied by irrigation. The additional energy supplied by enhanced SWF goes into evaporation, causing an increase in the LHF. Because more energy is used for evaporation near the diurnal peak, less is available for warming of the surface, and hence, SHF correspondingly decreases. Therefore, the repartitioning into SHF and LHF drives the bulk of the cooling seen in Figure 7. By irrigating, we increase the localized evaporation (Figure 6b), which in turn cools the surface, ultimately lowering the mean surface temperatures.

There is another interesting source of cooling in the irrigated runs: the decrease in ground heat flux (GHF; Figure 8e). The reduction indicates that in irrigated runs, more energy is being transferred from the top soil to the deep subsurface layers, which produces a slight warming of the deep soil layers (not shown). This is a less-discussed mechanism by which irrigation can affect surface temperatures. Further, the reductions to GHF

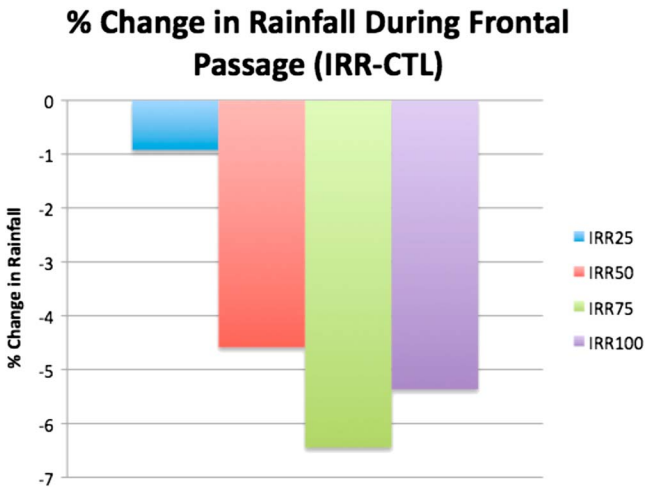


**Figure 11.** The percent change in rainfall accumulation averaged over all cultivated cells averaged across all frontal passage events. Results are found to be significant at the 10% confidence interval.

follow a similar consistent relationship as surface temperatures; that is to say, as irrigation vigor steadily increases, so too does the reduction to ground heat flux.

### 3.3. Impacts on Transient Frontal Passage

In the SEUS, transient frontal passages can occur in early May and late October (Figure 9) when the atmosphere is sufficiently baroclinic. Because of irrigation's impact on precipitation and the local thermal environment, we should expect that irrigation would exert an influence on frontal passage events. In order to assess this, a late October frontal passage was isolated within CTL (Figure 9). One day prior to the passage (Figure 9a), there was moderate precipitation in the region, with a large cell associated with the front in the extreme western portion of the domain. Conditions in the SEUS appeared to be dominated by an offshore high-pressure system off the coast. On the day of frontal passage over the irrigated cells in Alabama, Georgia, and the Carolinas, (Figure 9b) conditions worsened, bringing heavy rains on the order of $>$21 mm over the day and establishing a dominant low-pressure system over the central portion of the SEUS. Following the frontal passage across these irrigated cells, (Figure 9c) temperatures cooled substantially as the front moved over the Florida Peninsula.

We compared these conditions against those from the same time frame in IRR100 (Figure 10). In terms of frontal location and translation speed, characteristics varied very slightly compared to CTL. This implies that irrigation had very little effect on the spatial and temporal characteristics of this frontal passage. However, there was a marked change in the precipitation characteristics of the frontal passage over the irrigated cells. On the day of the passage, when the front encountered cultivated cells, there was a net reduction in precipitation relative to CTL (Figure 10) owing primarily to the increase in the local atmospheric stability from irrigation. As the front traveled further east of the irrigated cells, lifting mechanisms became more efficient and created rainfall. Because diabatic heating in the irrigation runs is modulated relative to CTL, a downstream gravity wave-like pattern in precipitation is observed in the differences (Figure 10b). This pattern is related to organized deep convection (as along a cold frontal boundary) generating long gravity waves and inertia-gravity waves downstream of it [*Lane and Knievel,* 2005] as a result of interaction between unstable convective motions and the stable environment [*Lane and Sharman,* 2006]. Because triggering of this gravity wave is delayed by the presence of irrigation due to its modulation of convection along the frontal boundary, it is not surprising that the map of precipitation change follows a gravity wave-like pattern. On the following day, a similar pattern is found, with reductions in precipitation downwind of the irrigated cells, which is also accompanied by an increase in precipitation relative to CTL farther downstream (Figure 10c).

In order to assure that these results are not specific to the event discussed above, the composite precipitation change over the irrigated cells was computed across several frontal passages. The frontal passage over a given irrigated cell was objectively determined as any time a temperature change of $-5$°C was recorded at the said irrigated cell over 1 day in the months of May and October (Figure 11). Adjusting this threshold downward (to $-8$°C, the lowest level at which there are at least 1000 samples for calculations) further reduces rainfall by 1 to 4 percentage points. It was found that the average change for all cases of frontal passage in our simulation was a net reduction, on the order of 5–10% relative to CTL, significant at the 10% confidence level following a Monte Carlo test. IRR25 reported the lowest decrease in precipitation, which is consistent with

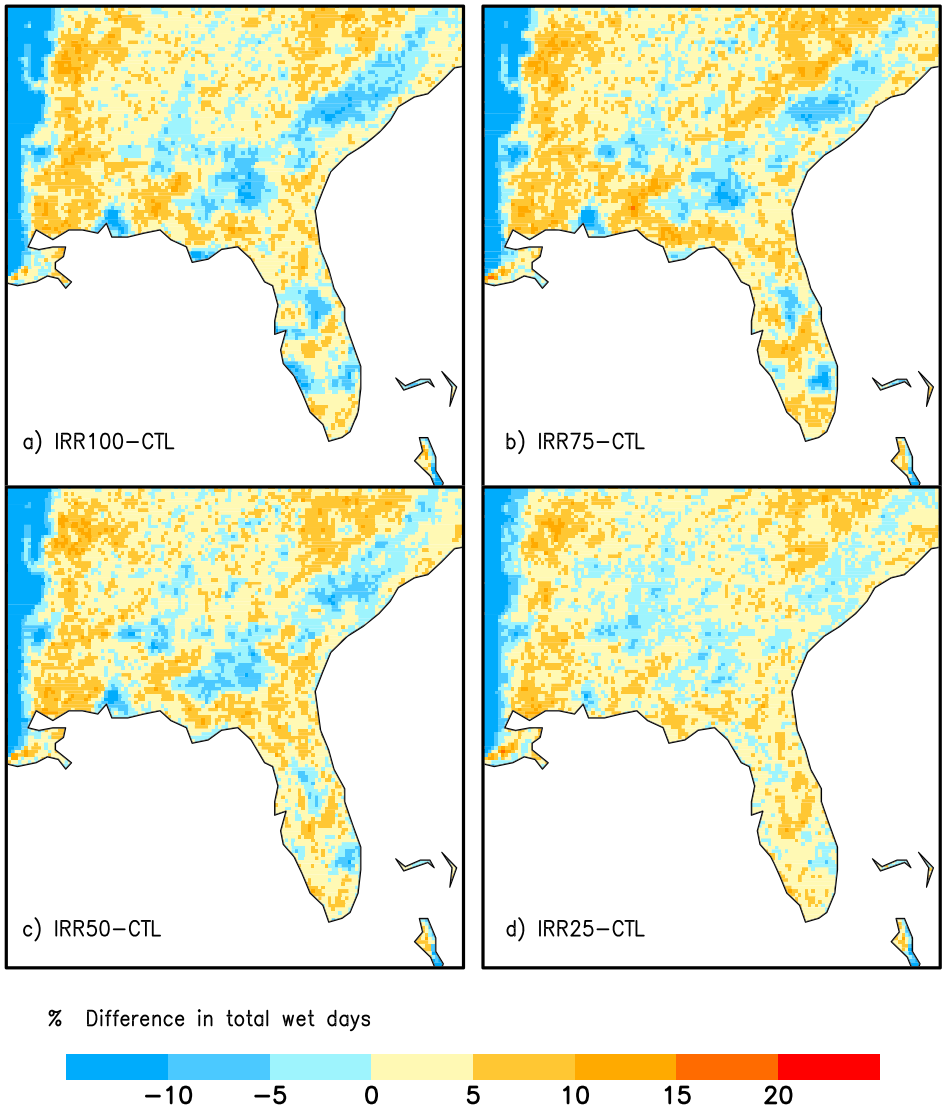


**Figure 12.** Percent reduction (IRR-CTL) in total number of wet days. Wet days are defined as days whose accumulated rainfall over a day total exceeds 1 mm.

results in section 3.1. IRR50, IRR75, and IRR100 were all within 2% of each other, with IRR75 reporting the largest reduction in rainfall.

### 3.4. Impacts on Dry Days and Heat Waves

Because irrigation has such a pronounced impact on climatological precipitation and temperature, we should expect that it manifests in meteorological events, including heat waves. One such aspect we are interested in is the geographical distribution of change in number of wet days. We consider days in which accumulated daily precipitation falls below (exceeds) 1 mm/d for dry days (wet days) [*Bastola and Misra,* 2013]. Using these definitions, we can then compute the percent difference in number of wet days (Figure 12). Again, we see a steady decrease in the influence of irrigation on the number of wet days as we reduce irrigation vigor; in IRR25, there is an unsubstantial reduction in the number of wet days with little spatial homogeneity. However, as irrigation vigor is increased, there is additional spatial coverage in reductions, and reduction magnitude becomes more pronounced. As such, we see that irrigation can be attributed for a worsening of water accumulation in an area, a somewhat ironic conclusion considering irrigations function in crop growth. This could potentially create difficulties in water storage for irrigation purposes, as a secondary source of irrigation water would considerably reduce.

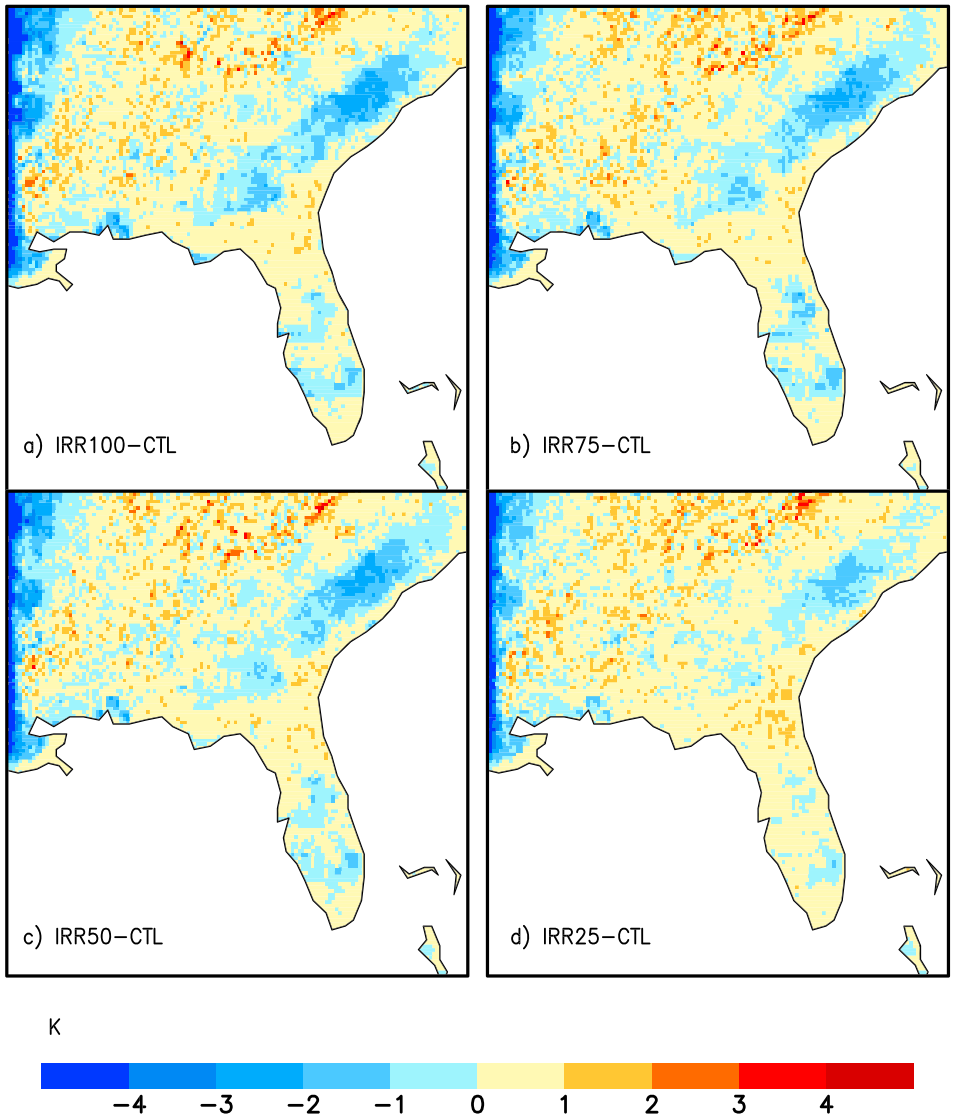


**Figure 13.** Difference (IRR-CTL) in threshold temperatures used in determining heat wave days. Thresholds are computed as the top 97.5th percentiles of all seasonal temperatures.

We then check to see if irrigation, which reduces local temperatures, has an impact on heat waves in an area. In order to do this, we define heat waves as three or more consecutive days in which the daily maximum temperature exceeds the 97.5th percentile of the seasonal temperatures in summer [*Russo et al.*, 2014]. Once we have done this, we then compute the difference in threshold temperature for each irrigation simulation (Figure 13). Irrigation indeed reduces the threshold temperature over the irrigated cells for what constitutes a heat wave substantially. Again, as with wet days, there is a steady increase in spatial coverage of the reduction; however, the magnitude does not seem to change significantly much past IRR50. While an increase in heat wave days with irrigation seems counterintuitive at the outset, it is important to note that the most significant aspect of a heat wave is its human impact. As the intensity of these new heat waves would be quite modest, akin to typical warm summer day temperatures, the human impact would be small. In fact, if we were to fix the threshold temperature to define the heat wave from the CTL run, then we would see a substantial reduction in the number of heat wave days over and near irrigated areas as the irrigation vigor increases (Figure 14). This reduction is helpful, as it reduces overall crop stress, of which temperature is a major contributor [*Kai and Iba*, 2014] which can in turn increase crop productivity and yield.

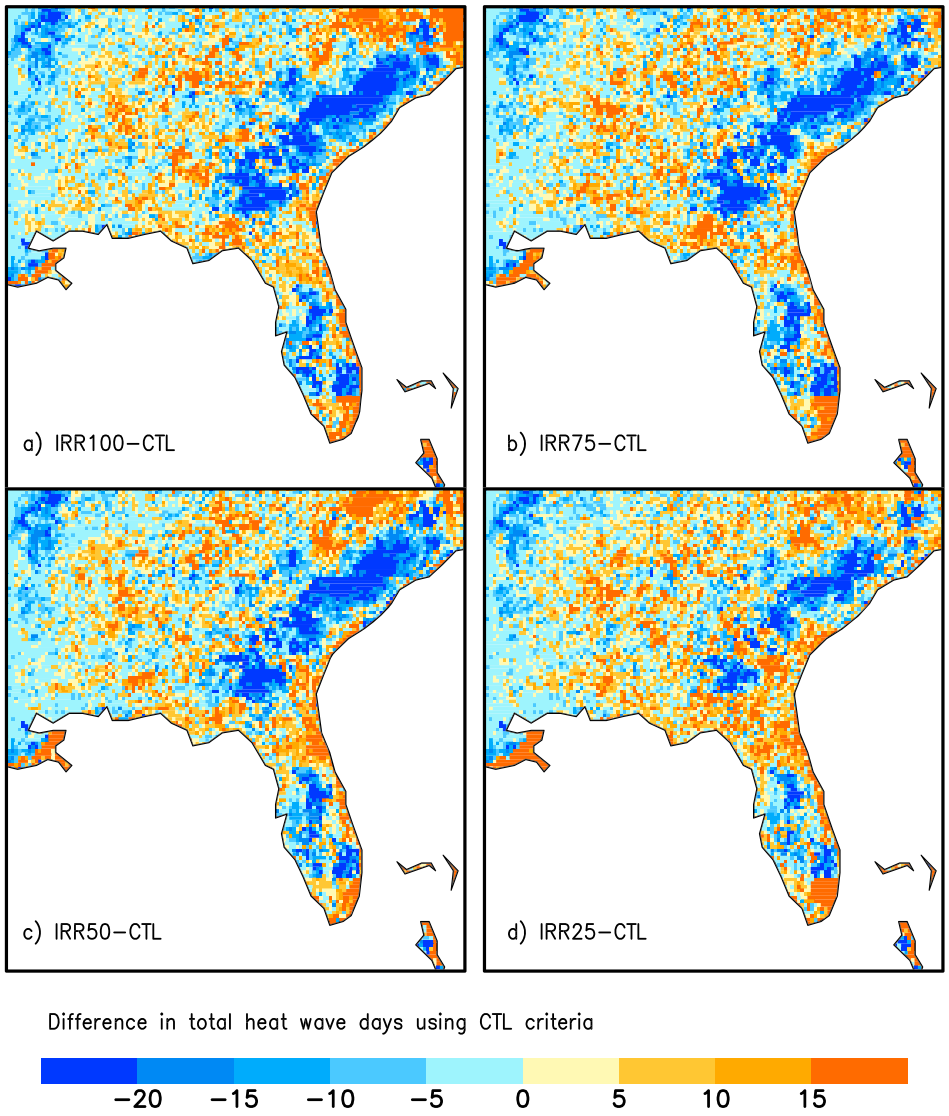


**Figure 14.** Difference (IRR-CTL) in total number of heat wave days using CTL threshold criteria.

## 4. Summary and Conclusions

A noted result of this study is that irrigation in the SEUS seems to cause a reduction in precipitation over the irrigated cells. This reduction seems to further with increase in irrigation vigor. At the outset this may seem rather counterintuitive. But like the tropics, the SEUS is moist neutral. In the absence of strong boundary forcing, convection remains capped during the summer time in the SEUS. By way of irrigation an immediate and obvious impact is the cooling of the surface, which leads to increasing the stability of the atmosphere in the boundary layer and thereby stymying convection.

The primary mechanism for reducing temperatures is a repartitioning of energy into latent heat flux, which drives cooling through evaporation. An additional source of cooling is downward transport of energy to the deep-soil layers through a reduced ground heat flux. The decrease in ground heat flux seems to change linearly as irrigation vigor increases. As irrigation vigor increases we find that there is a noticeable increase in 0–1 mm/d rainfall (dry day) events and decrease in $>$1 mm/d rainfall events. Irrigation also seems to have an impact on frontal passage in late May and early October. Local changes in atmospheric stability from irrigation tend to suppress precipitation over the irrigated cells. The fronts travel downwind of irrigated cells before their lifting mechanisms become more efficient. The net result of this change is a reduction in

precipitation over irrigated areas during frontal passage. In addition, increasing irrigation vigor promotes a decrease in number of wet days (days with accumulated rainfall greater than 1 mm) and a reduction in the threshold (and thus intensity) of heat wave events. Furthermore, we found that irrigation mitigates the intensity of heat waves. While few people live in areas where irrigation would occur, this is still significant, as heat waves tend to add to crop stress.

From our results we can conclude that first and foremost irrigation schemes must be assessed for their total water usage. Methods similar to the ones used in this study have been employed in other studies, yet few have monitored exactly how much water was used. A more realistic scheme, which only irrigates during the daytime, or perhaps keeps track of where the water is withdrawn will further improve upon this study's results. In addition, as computing power grows, additional runs could further enhance our understanding of the climate's sensitivity to irrigation vigor, associated crop rotations, changing land cover, and land use patterns to possibly help in optimal design of irrigation systems.

**Acknowledgments**
This work was supported by grants from NOAA (NA12OAR4310078, NA10OAR4310215, and NA10OAR4320143) and USGS G13AC00408. All model integrations for this paper were done on the computational resourced provided by the Extreme Science and Engineering Discovery Environment (XSEDE) under TG-ATM120010. Data used in this study are available upon request from corresponding author at cms05j@my.fsu.edu.

## References

Alston, J. M., B. A. Babcock, and P. G. Pardey (2010), Introduction and overview, in *The Shifting Patterns of Agricultural Production and Productivity Worldwide. CARD MATRIC Electronic Book*, chap. 1, edited by J. M. Alston, B. A. Babcock, and P. G. Pardey, 1–6 pp., Cent. for Agric. and Rural Dev., Ames, Iowa. [Available at http://www.matric.iastate.edu/shifting_patterns/.]

Alter, R. E., Y. Fan, B. R. Lintner, and C. P. Weaver (2015), Observational evidence that Great Plains irrigation has enhanced summer precipitation intensity and totals in the midwestern United States, *J. Hydrometeorol.*, *16*, 1717–1735.

Barnston, A. G., and P. T. Schickedanz (1984), The effect of irrigation on warm season precipitation in the Southern Great Plains, *J. Climate Appl. Meteorol.*, *23*, 865–888.

Bastola, S., and V. Misra (2013), Seasonal hydrological forecasts for watersheds over the southeastern United States for the boreal summer and fall seasons, *Earth Interact.*, 17, 25, doi:10.1175/2013EI000519.1.

Cook, B. I., S. P. Shukla, M. J. Puma, and L. S. Nazarenko (2015), Irrigation as an historical climate forcing, *Clim. Dyn.*, *44*, 1715–1730.

Cosgrove, B., et al. (2003), Real-time and retrospective forcing in the North American Land Data Assimilation System (NLDAS) Project, *J. Geophys. Res.*, *108*(D22), 8842, doi:10.1029/2002JD003118.

DeAngelis, A., F. Dominguez, Y. Fan, A. Robock, M. D. Kustu, and D. Robinson (2010), Evidence of enhanced precipitation due to irrigation over the Great Plains of the United States, *J. Geophys. Res.*, *115*, D15115, doi:10.1029/2010JD013892.

Ek, M. B., K. E. Mitchell, Y. Lin, E. Rogers, P. Grunmann, V. Koren, G. Gayno, and J. D. Tarpley (2003), Implementation of NOAH land surface model advances in the National Centers for Environmental Prediction operational mesoscale ETA model, *J. Geophys. Res.*, *108*(D22), 8851, doi:10.1029/2002JD003296.

Evett, S., D. Carman, and D. Bucks (2003), Expansion of irrigation in the mid South United States: Water allocation and research issues, in *2nd International Conference on Irrigation and Drainage, Water for a Sustainable World—Limited Supplies and Expanding Demand*, pp. 247–260, U.S. Comm. on Irrig. and Drain., Phoenix, Ariz.

Hagemann, S., and T. Stacke (2015), Impact of the soil hydrology scheme on simulated soil moisture memory, *Clim. Dyn.*, *44*, 1731–1750.

Harding, K., and P. Snyder (2012), Modeling the atmospheric response to irrigation in the Great Plains. Part I: General impacts on precipitation and the energy budget, *J. Hydrometeorol.*, *13*, 1667–1686.

Hutson, S., N. Barber, J. Kenny, K. Linsey, D. Lumia, and M. Maupin (2000), Estimated use of water in the United States in 2000, USGS Circular 1268, revised Feb. 2005.

Im, E.-S., and E. A. B. Eltahir (2014), Enhancement of rainfall and runoff upstream from irrigation location in a climate model of West Africa, *Water Resour. Res.*, *50*, 8651–8674, doi:10.1002/2014WR015592.

Im, E.-S., M. P. Marcella, and E. A. B. Eltahir (2014), Impact of potential large-scale irrigation on the West African Monsoon and its dependence on location of irrigated area, *J. Clim.*, *27*, 994–1009.

Jacob, D., et al. (2014), EURO-CORDEX: New high-resolution climate change projections for European impact research, *Reg. Environ. Change*, *14*, 563–578.

Kai, H., and K. Iba (2014), Temperature stress in plants, *eLS*, doi:10.1002/9780470015902.a0001320.pub2.

Kain, J., and M. Fritsch (1993), Convective parameterization for mesoscale models: The Kain-Fritsch scheme, *Meteorol. Monogr.*, *24*, 165–170.

Kanamaru, H., and M. Kanamitsu (2007), Scale selective bias correction in a downscaling of global analysis using a regional model, *Mon. Weather Rev.*, *135*, 334–350.

Kanamaru, H., and M. Kanamitsu (2008), Model diagnosis of nighttime minimum temperature warming during summer due to irrigation in the California Central Valley, *J. Hydrometeorol.*, doi:10.1175/2008JHM967.1.

Kanamitsu, M., W. Ebisuzaki, J. Woollen, S. K. Yang, J. J. Hnilo, M. Fiorino, and G. L. Potter (2002), NCEP DOE AMIP II reanalysis (R2), *Bull. Am. Meteorol. Soc.*, *83*, 1631–1643.

Kanamitsu, M., K. Yoshimura, Y. Yhang, and S. Hong (2010), Errors of interannual variability and trend in dynamical downscaling of reanalysis, *J. Geophys. Res.*, *115*, D17115, doi:10.1029/2009JD013511.

Kueppers, L., and M. Snyder (2012), Influence of irrigated agriculture on diurnal surface energy and water fluxes, surface climate and atmospheric circulation in California, *Clim. Dyn.*, *38*, 1017–1029.

Lane, T. P., and J. C. Knievel (2005), Some effects of model resolution on simulated gravity waves generated by deep mesoscale convection, *J. Atmos. Sci.*, *62*, 3408–3419.

Lane, T. P., and R. D. Sharman (2006), Gravity wave breaking, secondary wave generation, and mixing above deep convection in a three-dimensional cloud model, *Geophys. Res. Lett.*, *33*, L23813, doi:10.1029/2006GL027988.

Lin, Y., and K. E. Mitchell (2005), The NCEP Stage II/IV hourly precipitation analyses: development and applications, paper 1.2 presented at 19th Conference on Hydrology, Am. Meteorol. Soc., San Diego, Calif., 9–13 Jan.

Lo, M.-H., and J. S. Famiglietti (2013), Irrigation in California's Central Valley strengthens the Southwestern U.S. water cycle, *Geophys. Res. Lett.*, *40*, 301–306, doi:10.1002/grl.50108.

Lobell, D., G. Bala, A. Mirin, T. Phillips, R. Maxwell, and D. Rotman (2009), Regional differences in the influence of irrigation on climate, *J. Clim.*, *22*, 2248–2255.
Loveland, T. R., J. W. Merchant, B. C. Reed, J. F. Brown, D. O. Ohlen, P. Olson, and J. Hutchinson (1995), Seasonal land cover regions of the United States, *Ann. Assoc. Am. Geogr.*, *85*, 339–355.
Marcella, M. P., and E. A. B. Eltahir (2014), Introducing an irrigation scheme to a regional climate model: A case study over West Africa, *J. Clim.*, *27*, 5708–5723.
McNally, A., et al. (2004), Assessing the region via indicators: The economy, Great Valley Center special report.
McNider, R. T., and J. Christy (2007), Let the East bloom again, *New York Times Op-Ed*, Sept. 22.
McNider, R. T., J. Christy, and J. Hairston (2005), Bringing agriculture back to water—A solution for the 21st century, in *Proceedings of the AMS Forum: Living With a Limited Water Supply, Annual Meeting of the American Meteorological Society*, sect. 2.4. [Available at https://ams.confex.com/ams/Annual2005/techprogram/paper_85724.htm.]
Misra, V., and P. A. Dirmeyer (2009), Air, sea, and land interactions of the continental U.S. hydroclimate, *J. Hydrometeorol.*, *10*, 353–373.
Misra, V., J.-P. Michael, R. Boyles, E. P. Chassignet, M. Griffin, and J. J. O'Brien (2012), Reconciling the spatial distribution of the surface temperature trends in the southeastern United States, *J. Clim.*, *25*, 3610–3618.
Parker, M. D., and D. A. Ahijevych (2007), Convective episodes in the east-central United States, *Mon. Weather Rev.*, *135*, 3707–3727.
Puma, M., and B. Cook (2012), Effects of irrigation on global climate during the 20th century, *J. Geophys. Res.*, *115*, D16120, doi:10.1029/2010JD014122.
Qian, Y., M. Y. Huang, B. Yang, and L. K. Berg (2013), A modeling study of irrigation effects on surface fluxes and land-air-cloud interactions in the Southern Great Plains, *J. Hydrometeorol.*, *14*, 700–721.
Russo, S., A. Dosio, R. G. Graversen, J. Sillmann, H. Carrao, M. B. Dunbar, A. Singleton, P. Montagna, P. Barbola, and J. V. Vogt (2014), Magnitude of extreme heat waves in present climate and their projection in a warming world, *J. Geophys. Res. Atmos.*, *22*, 12,500–12,512, doi:10.1002/2014JD022098.
Sacks, W., B. Cook, N. Buenning, S. Levis, and J. Helkowski (2009), Effects of global irrigation on the near-surface climate, *Clim. Dyn.*, *33*, 159–175.
Saeed, F., S. Hagemann, and D. Jacob (2009), Impact of irrigation on the South Asian summer monsoon, *Geophys. Res. Lett.*, *36*, L20711, doi:10.1029/2009GL040625.
Schaible, G. D., and M. P. Aillery (2012), Water conservation in irrigated agriculture: Trends and challenges in the face of emerging demands, USGS EIB-99, 67 pp.
Schwartz, B. E., and L. F. Bosart (1979), The diurnal variability of Florida rainfall, *Mon. Weather Rev.*, *107*, 1535–1545.
Selman, C. (2015), Simulating the impacts and sensitivity of the southeastern United States climatology to irrigation, 101 pp., Dep. of Earth, Ocean and Atmos. Sci., Fla. State Univ. [Available at http://diginole.lib.fsu.edu/islandora/object/fsu:253136/datastream/PDF/view.]
Selman, C., and V. Misra (2015), Simulating diurnal variations over the southeastern United States, *J. Geophys. Res. Atmos.*, *120*, 180–198, doi:10.1002/2014JD021812.
Selman, C., V. Misra, and L. Stefanova (2013), On the twenty-first century wet season projections over the southeastern United States, *Reg. Environ. Change*, *13*, S153–S164, doi:10.1007/s10113-013-0410-1.
Shukla, S. P., M. J. Puma, and B. I. Cook (2014), The response of the South Asian Summer Monsoon circulation to intensified irrigation in global climate model simulations, *Clim. Dyn.*, *42*, 21–36.
Sorooshian, S., J. Li, K.-L. Hsu, and X. Gao (2011), How significant is the impact of irrigation on the local hydroclimate in California's Central Valley? Comparison of model results with ground and remote-sensing data, *J. Geophys. Res.*, *116*, D06102, doi:10.1029/2010JD014775.
Uppala, S. M., et al. (2005), The ERA-40 re-analysis, *Q. J. R. Meteorol. Soc.*, *131*, 2961–3012, doi:10.1256/qj.04.176.
Vories, E. D., and S. R. Evett (2010), Irrigation research needs in the USA mid-south and Southeast, humid and subhumid regions, paper IRR10-8679 presented at Proceedings for the 5th National Decennial Irrigation Conference ASABE.
Wei, J., and P. Dirmeyer (2012), Dissecting soil moisture-precipitation coupling, *Geophys. Res. Lett.*, *39*, L19711, doi:10.1029/2012GL053038.
Wilkes, D. (2011), *Statistical Methods in the Atmospheric Sciences*, 2nd ed., 704 pp., Academic Press, Burlington, Mass.
Zobler, L. (1986), A world soil file for global climate modeling, NASA Technical Memorandum 87802.